www.cadanda.com
Computer-Aided Design AND APPLICATIONS

Digital Bas-Relief Design: a Novel Shape from Shading-Based Method

Lapo Governi[1], Monica Carfagni[2], Rocco Furferi[3], Luca Puggelli[4] and Yary Volpe[5]

[1]Department of Industrial Engineering, University of Florence – Italy, lapo.governi@unfi.it
[2]Department of Industrial Engineering, University of Florence – Italy, monica.carfagni@unfi.it
[3]Department of Industrial Engineering, University of Florence - Italy, rocco.furferi@unifi.it
[4]Department of Industrial Engineering, University of Florence – Italy, luca.puggelli@unifi.it
[5]Department of Industrial Engineering, University of Florence – Italy, yary.volpe@unifi.it

ABSTRACT

Design of products characterized by high stylistic content and organic shapes in the form of bas-relief (e.g. fashion accessories, commemorative plaques and coins) is traditionally performed starting from handmade drawings or photographs that are manually reproduced by highly skilled craftsmen such as sculptors and engravers and finally digitized by means of 3D scanning. Several Computer-based procedures have been devised with the aim of speeding up this process, which is considerably time consuming, subjective and costly; these are mainly based on image processing techniques such as embossing, enhancement, histogram equalization or dynamic range, also implemented in CAD-based commercial software. However, these approaches are characterized by several limitations preventing them from providing a "correct" final geometry. In view of that, the present work describes a novel method for the creation of digital bas-reliefs from a single image using a Shape From Shading (SFS) based approach with interactive initialization. Image processing-based techniques and minimization SFS methods are first used in order to retrieve a rough version of the objective surface; successively, this is used as initialization for the final reconstruction algorithm. Tested on a set of case studies, the method proved to be effective in providing satisfactory digital bas-relief from single images.

Keywords: digital bas-relief, shape retrieval, shape from shading, image processing.

1. INTRODUCTION

For products characterized by high stylistic content and organic shapes (such as jewels, fashion accessories, ceramics, house-ware, plaques and coins), design process often starts from handmade drawings, photographs or images in general which are traditionally reproduced by craftsmen in the form of relief or bas-relief. Handmade bas-relief manufacture is usually carried out by highly skilled operators (e.g. sculptors and engravers). This process is highly subjective, costly, time-consuming and the obtained reliefs are hard to modify, to repair and to reproduce [29]. These drawbacks become critical when cost and time to market are a crucial issue for the manufacturer and, all the more, when several alternatives are to be considered before ultimate product definition.

In order to confront with these issues, in the last few years a number of Computer-based methods have been devised with the aim of speeding up the relief reconstruction process from single images.

The final result of these techniques usually consists of a "digital relief" to be used as input for CAM and/or RP systems.

A digital relief conveys a volumetric projection of the design shapes into the viewer's space (thus detaching itself from the two dimensional background) [15]. The methods aimed to create such a representation broadly fall into the area of computer aided 3D modeling from single images, for which different approaches have been proposed in literature [19,22,25]. The main issue in the retrieval of the 3D shape represented in a single image is that it results in an ill-posedness of problem; accordingly, literature works are mostly aimed to solve it under certain circumstances, often by using user interaction.

Image embossing [12] is, still today, one of the most common approaches for recovering a digital relief from single image; embossing an image is a computer graphics technique in which each pixel of an image is replaced either by a highlight or a shadow,

Taylor & Francis

depending on boundaries on the original image. The obtained result is a fake relief since it only visually resembles a bas-relief with a very shallow and incorrect depth (due to the algorithm based on image gradient computation).

Alternative techniques, like the one proposed by Weyrich et al. [30] and by Sun et al. [26], just to cite a few, improved the embossing method by using preprocessing techniques based on image enhancement, histogram equalization and dynamic range.

Unsharp masking and smoothing have also been combined in order to emphasize salient features and deemphasize others in the original image [26].

In a recent paper [18] an approach for estimating the height map from single images representing brick and stone reliefs (BSR) has been proposed. The method proved to be adequate for restoring BSR surfaces by using a height map estimation scheme consisting of two levels: the bas-relief, referring to the low frequency component of the BSR surfaces, and the high frequency detail. However, due to the assumption of BSR priors, the method proves to be unsatisfactory when the relief of surface to be retrieved increases with respect to typical BSR surfaces.

Commercial software, like ArtCAM and JDPaint [29] have been also developed making available functions for 3D bas-relief reconstruction. These software packages basically consist of CAD modelers where (heavy) user interaction is a crucial task both in the pre and in the post-processing phases. Generally speaking, the relief is generated starting from an image which is already a height map of the object (in this case the input is not a real image but, rather, a 3D surface) or by using as a height map the image resulting from derivative-based operators applied to the starting image itself (i.e. the result of image embossing). As an alternative, commercial software allow to use vector representation of the object to be reconstructed and "inflate" the surface delimited by the object outlines (this procedure will be referred to in the rest of the paper using the term inflation [13,23]. A combination of inflation and either direct image height map or image embossing is also possible. A few examples of these techniques are presented in the section describing the case studies at the end of the paper.

Shape From Shading (SFS) techniques, extensively studied in the last decades, also have the potential of producing a 3D model from a single intensity image. SFS is a computational approach that bundles a number of techniques aimed to reconstruct the three-dimensional shape of a surface shown in a single grey-level image. Extensively reviewed by [6,34], SFS methods are based on the theory that the intensity of a pixel is proportional to the angle between the surface normal and the lighting direction. A particularly significant work in the field of bas-relief reconstruction from single image is presented by Wu et al. in [32]. This work presents an interesting approach based on the combination of SFS and artificial intelligence techniques. The main idea is to teach a learning algorithm how to reproduce the bas-relief image corresponding to a given one and then to apply a modified SFS algorithm to the new image. Though the approach looks very promising and the results are encouraging, it can be applied only to specific categories of objects which have been used for training the learning algorithm (human faces from frontal photograph in the case of the aforementioned paper).

Generally speaking, however, automatic shape retrieval using SFS techniques proves to be unsuitable for producing high-quality bas-reliefs [29]. As a consequence, recent improvement have been obtained by implementing interactive methods [4,33] where the user is required to specify absolute surface positions or absolute surface normals as constraints. In particular [33] proposed a two-step procedure; the first step recovers high frequency details using SFS. The second step corrects low frequency errors using a user-driven editing tool.

However, this approach entails quite a considerable amount of user interaction especially in the case of complex geometries. Nevertheless, in case the amount of required user interaction can be maintained at a reasonable level, interactive SFS methods may be considered among the best candidate techniques for generating high quality bas-reliefs starting from single images.

Moving from these considerations, this work is aimed to propose a novel method for creation of digital bas-reliefs starting from single images using a SFS technique with interactive initialization.

Image processing-based techniques and minimization SFS methods are first used in order to retrieve a rough version of the objective surface; successively, this is used as initialization for the final reconstruction algorithm. Both the phases are based on Gauss-Seidel iteration with Successive Over Relaxation (SOR). The whole process is graphically summarized in Fig. 1.

2. METHOD

With the aim of reconstructing (in the form of bas-relief) the shape of a subject represented in a single image, a methodology consisting of the following 3 steps is proposed (steps 2a and 2b represent two alternatives):

1) Definition of a suitable error functional between a given surface and the expected one.
2a) Retrieval of a rough solution (surface) by minimizing an over-smoothed version of the functional (Simplified Method, from now on SM).
2b) Retrieval of a rough solution (surface) by combining image processing-based methods and SFS (Image Processing-based Method, from now on IPM).

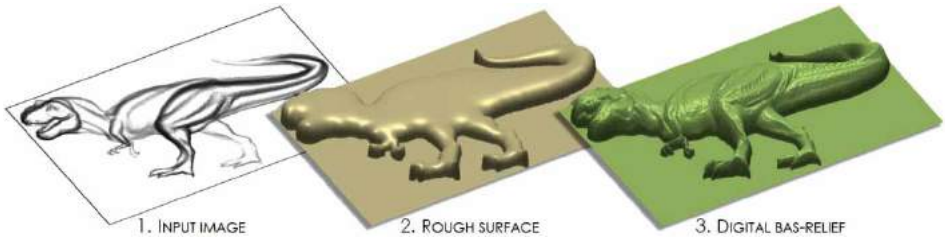

Fig. 1: Process for creation of digital bas-reliefs starting from single images using a SFS technique.

3) Retrieval of final surface using the rough solutions as initialization function for the SFS main reconstruction problem.

2.1. Functional Definition

Under the hypotheses that: the surface to be reconstructed is completely diffusive (i.e. Lambertian), the albedo is constant in all the reconstruction domain, the light source is set at infinity and image is free from perspective distortion, the formulation of the problem is provided by the following, widely known, equation often referred as "SFS problem" [10]:

$$\vec{L} \cdot \vec{N} = \frac{1}{\rho} I \tag{2.1}$$

where $\vec{L} = [l_x, l_y, l_z]$ is the unit-vector opposed to light direction, $\vec{N} = [n_x, n_y, n_z]$ is the outward unit-length vector normal to the surface (unknown of the problem), ρ is the albedo and I is the brightness.

Generally speaking, it is possible to identify four different approaches aiming at solving the above mentioned SFS problem (i.e. Eqn. 2.1): direct methods [16,21,24], minimization methods [4,5,7,9,11,14,31, 33], local approximation methods [17,20] and linear approximation methods [27]. Among them, minimization methods seem to provide the right compromise between efficiency and flexibility, since they lead to quite good results also starting from noisy images or imprecise settings (e.g. guessed light direction when unknown). Minimization methods are based on the hypothesis that the expected (reconstructed) surface is the one that minimizes a suitable functional, composed by the sum of several contributions (called "constraints") and usually representing the error between the (iteratively) reconstructed surface and the expected one.

In the present work, such a functional is built according to [8]; in detail, it is obtained as a linear combination of brightness and smoothness constraints, as follows:

$$\begin{aligned} E = & B + \lambda S = \sum\nolimits_{i \epsilon D} \left(1/\rho I_i - \vec{N}_i^T \cdot \vec{L}\right)^2 \\ & + \lambda \sum\nolimits_{\{i,j\} \in D} (\vec{N}_i - \vec{N}_j)^2 \end{aligned} \tag{2.2}$$

where i is the pixel index, j is the index of a generic pixel belonging to the 4-neighbourhood of pixel I, I_i is the brightness of pixel i (range [0-1]), $\vec{N}_i = [n_{i,x}, n_{i,y}, n_{i,z}]$ and $\vec{N}_j = [n_{j,x}, n_{j,y}, n_{j,z}]$ are the unit length vectors normal to the surface (unknown) in positions i and j, respectively and λ is a regularization factor for smoothness constraint (weight).

Since E is quadratic, it can be expressed in a matrix form as follows:

$$\begin{cases} E = \frac{1}{2} \Phi^T A \Phi + \Phi^T b + c \\ \Phi = [n_{1,x}, n_{2,x}, \ldots, n_{k,x}, n_{1,y}, n_{2,y}, \ldots, n_{k,y}, n_{1,z}, \\ \qquad n_{2,z}, \ldots, n_{k,z}]^T \end{cases} \tag{2.3}$$

where k is the total number of pixels, A is a $3k \times 3k$ matrix, b is a $3k$ vector and c is the constant term. In practice, vector Φ is a re-arrangement of the surface normal map.

Moreover, since its gradient $\nabla(E)$ is linear (Eqn. 2.4), its minimization is extremely fast, and it makes preferable to use indirect minimization process instead of direct ones.

$$\nabla(E) = A\Phi + b \tag{2.4}$$

In order to conveniently minimize the functional, a number of specific boundary conditions (BCs from now on) can be imposed so as to bind the research to surfaces which satisfy certain requirements. In other words, when it is possible to figure out or, more in general, to define a priori some "features" of the shape represented in the image, suitable constraints can be set in order to guide the minimization process towards the expected surface. A number of works (see the above cited minimization methods) have been carried out in order to devise automatic or user-based methods to impose BCs. Among these methods, user-guided ones proved to be the most effective, since human interaction can be discriminant in a number of ambiguous cases (e.g. to discriminate local maxima and minima). As a consequence, in the present work, a user-based procedure has been adopted for imposing BCs. The description of this procedure, extensively discussed in [8], is beyond the scope of the present work; in fact, the main interest here is not to describe how to impose BCs but rather to use a suitable set of BCs with the aim of reconstructing a rough version of the expected surface.

The BCs taken into account in this work are the following ones: *background*, *singular points*, *silhouette contour* and *morphology based BC* [2,8,14].

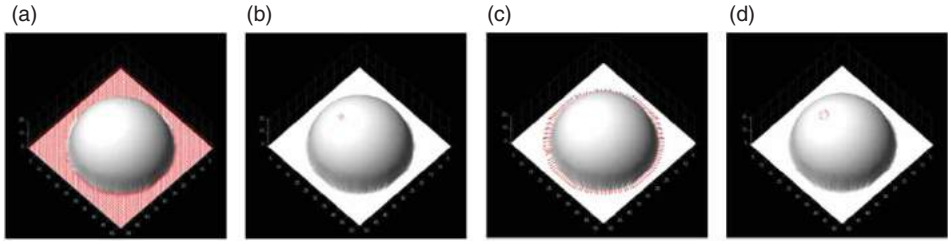

Fig. 2: Examples of boundary condition: (a) *Background*; (b) *Singular Points*; (c) *Silhouette Contour*; (d) *Morphology Based*.

- *Background boundary condition* (Fig. 2a); it consists of setting unit length normal vector for all the pixels belonging to the background of the scene, so that it will be perfectly horizontal once reconstructed.
- *Singular points boundary condition* (Fig. 2b); it consists of setting a proper value to the unit normal for all the singular points of the image, i.e. for all the white pixels. In fact, for such pixels the only possible unit normal vector is the one coincident with $\vec{L}$. Being the image brightness defined as the dot product between the two unit vectors $\vec{N}$ and $\vec{L}$, brightness reaches its maximum value when such vectors are parallel. In fact, referring to z_{light}, defined as the Z axis direction parallel to the unit vector $\vec{L}$, white pixels necessarily match with stationary points (i.e. maxima, minima or saddle points).
- *Silhouette contour boundary condition* (Fig. 2c); it consists of setting the unit normals, in correspondence of the pixels belonging to the boundary of the subject represented in the image, as outward-pointing. This particular BC is meant to facilitate the "rough" reconstruction of the overall volume of the shape, similarly to what commercial software do.
- *Morphology based boundary condition* (Fig. 2d); this BC, devised by the authors, allows to discriminate if a white region of the image corresponds to maxima or minima respect to z_{light}. Defining Π_{light} as the generic plane normal to z_{light}, if a white region of the image corresponds to a maximum or a minimum, the projection on Π_{light} of the unit normals belonging to the region boundary are, respectively, outward or inward pointing. This assumption guides the minimization process to reconstruct a surface whose maxima and minima are properly discriminated (this solves one of the typical SFS problem, which is the concave-convex ambiguity).

Once the BCs are set, the number of variables is reduced and the functional to be minimized needs to be modified accordingly. The (new) reduced matrix formulation of the gradient can be defined as follows:

$$\nabla(E_r) = A_r\hat{\Phi} + b_r \tag{2.5}$$

Where E_r, A_r, b_r and $\hat{\Phi}$, and are the reduced versions of, respectively, E, A, b and Φ.

In other words, two main effects are achieved: 1) reduction of the overall number of variables and 2) setting of appropriate constraints to the surface retrieval procedure. One of the main drawbacks of direct minimization is that, often, they lead to the nearest local minimum instead of the global one. This is the reason why, actually, these methods are effective only when the function to be minimized is strictly convex. Minimization algorithms usually need to be initialized: this process, in practice, consists of imposing an initial guess to the solution. Since we are dealing with variables representing unit normal components, this is usually accomplished using values which are either corresponding to planes or random. However, these kinds of initialization may lead to unreliable reconstruction due to the fact that expected solution can be considerably different from the starting one (i.e. distant in the variable domain). In fact, in minimization problems of not strictly convex functions, a smart way of solving the problem is to impose a convenient initialization to the unknowns in order to "reduce", as much as possible, the distance between the starting point and the expected solution. Hence, a remarkable issue is to understand whether, starting from a reconstructed surface that is roughly similar to the expected one, the minimization is effectively "guided" to converge to a better final solution than the one obtainable with conventional initialization. As a consequence a method for providing a better initial solution for the minimization procedure is highly advisable. Accordingly, as also stated in the introductory section, two approaches meant to obtain a suitable initial solution for the minimization procedure are provided below. Both the methods are based on Gauss-Seidel iteration with Successive Over Relaxation – SOR [1]:

- *Simplified SFS Method (SM).* Starting from the input image I, a number of BCs are imposed and the SOR – based minimization is performed setting high values for the smoothness constraint (e.g. $\lambda = 10^2$). The method allows to obtain a very smooth surface denoted with S^0_{SM}.

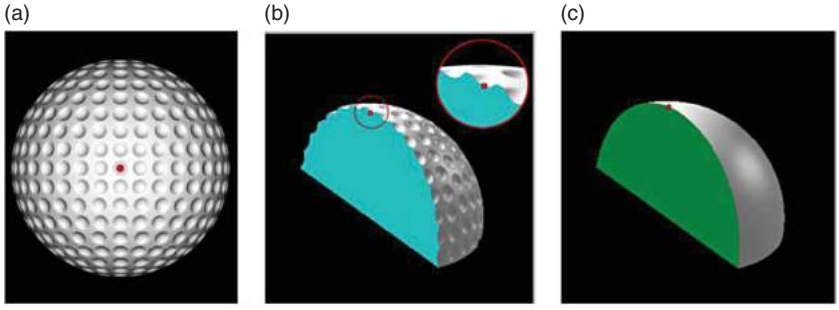

Fig. 3: (a) User-selected point on the input image; (b) correspondence of the selected point on the actual surface, local minimum; (c) correspondence of the selected point on the rough surface, global maximum.

– *Image Processing-based Method (IPM).* The input image I is modified using image processing based techniques with the aim of suppressing high-frequency details. SOR minimization method is, then, applied by imposing all the required BCs and using default settings for the smoothness constraint (e.g. $\lambda = 10^{-2}$). Also in this case, the final result consists of a very smooth surface denoted with S^0_{IPM}.

Actually, in both cases, the minimization process provides a normal map which needs to be further processed in order to obtain a geometrically feasible surface. This is no trivial task and is investigated by a number of researchers all over the world. For the moment, it needs to be pointed out that the normal map of a generic surface S does not always coincide with the one (Φ^{temp}) used for computing S: this is true only if Φ^{temp} is such that the same height is reached whatever the integration path [7]. Let us assume that S^0_{SM} and S^0_{IPM} are the surfaces which can be obtained starting from the normal maps provided by the two methods described above (further details about this step will be provided in the following section); due to the reason mentioned before, such surfaces are characterized by normal maps Φ^{start}_{SM} and Φ^{start}_{IPM} which are generally different from the original ones. Φ^{start}_{SM} and Φ^{start}_{IPM} are the normal maps used, alternatively, for initializing the Functional of Eqn. 2.1 in order to retrieve, by solving the main reconstruction problem, two final surfaces (respectively, S_{SM} and S_{IPM})).

2.2. Simplified SFS Method (SM)

As previously stated, the main aim of this method is to obtain a rough version of the desired surface to be retrieved. As a consequence, it is necessary to identify the common features that such a rough surface will share with the desired one. First, the rough surface can be envisaged as a sort of "inflation" of the region bounded by silhouette contour, in fact the goal of the this work is to obtain a bas relief-like surface, emerging from a flat background. Therefore, *silhouette contour BC* has to be imposed.

Moreover, both the surfaces (rough and desired one) necessarily share also the same overall morphology. As a consequence, a straightforward method is to apply the *morphology based BC* on a convenient subset of the singular points (i.e. white pixels) of the input image. In detail, the user should select and classify (as maxima or minima) the singular points in the image more closely characterizing the global geometry. Referring to the example of Fig. 3a, the user will select and classify as a maximum the singular point marked in red since the expected rough surface is an hemisphere, even if such a point is a local minimum of the expected final surface.

Dealing with the third BC (*background BC*), it is always used (imposed) since, as already stated for the *silhouette contour BC*, a surface emerging from a flat background is sought.

Finally, the two surfaces do not necessarily share all the singular points (as in the example provided in Fig. 3); hence, it is not usually possible to impose the *singular point BC*.

Once the BCs are imposed, Eqn. 2.5 can be minimized using the SOR algorithm and a planar normal map as initialization.

The solution, consisting of a normal map Φ^{temp}_{SM}, is provided using a high regularizing factor λ for smoothness constraint (e.g. $\lambda \geq 10^2$).

Starting from Φ^{temp}_{SM}, the surface is evaluated by minimizing (again by SOR algorithm) the following functional:

$$E_2 = \sum\nolimits_{\{i,j\}} ((z_i - z_j) - q_{ij})^2 \tag{2.6}$$

where z_i and z_j are respectively the heights relative to pixel i and j, while q_{ij} is the relative height between the two points, calculated by fitting an osculating arc between the two normals $\vec{N}_{\text{i}}$ and $\vec{N}_{\text{j}}$ [33].

The entire set z_i of values defines a surface S^0_{SM} that may be considered a low-frequency version of the desired one, thus appearing very smooth.

2.3. Image Processing-Based Method (IPM)

A low-frequency version of the desired surface may be also obtained using the alternative method (IPM),

under the hypothesis that the image relative to the rough shape is directly retrievable from the given one. This can be easily carried out by adopting well known digital image processing techniques. Many filters developed and commonly used for digital image processing, can be extremely useful to this purpose. Probably the best filter to cope with the necessity of reducing the high frequency content of an image is the Gaussian smoothing filter.

The Gaussian filter is a $k \times k$ convolution operator whose elements reproduce a weighted average characterized by a Gaussian distribution with σ standard deviation. One of the principal justifications for using such operator is due to its frequency response: in fact it acts as a low-pass filter, thus removing high spatial frequency components from the image. k value depends on the dimensions of the image I to be processed. Let $n \times m$ be the size of the image I, k is obtained as follows:

$$k^2 = int[v \cdot m \cdot n] \tag{2.7}$$

where v is a scale factor; the greater the value of v, the smoother the resulting image. In Fig. 4, the image $\tilde{I}$ obtained by using a Gaussian filter with $\sigma = 0.5$ and $k = 28$ ($v = 0.5 \cdot 10^{-2}$) is shown.

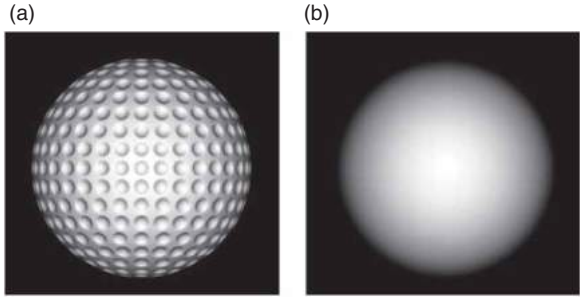

Fig. 4: (a) Input image, 407 x 407 pixel^2; (b) filtered image using a 28 x 28 pixel^2 Gaussian filter.

Once the filtered image $\tilde{I}$ is obtained, it is possible to solve the SFS problem using the following formulation:

$$\tilde{E} = \tilde{B} + \lambda \tilde{S} = \sum_{i \epsilon D} (1/\rho \tilde{I}_i - \vec{N}_i^T \cdot \vec{L})^2 + \lambda \sum_{\{i,j\} \in D} (\vec{N}_i - \vec{N}_j)^2 \tag{2.8}$$

where $\tilde{E}$ is the functional applied to the transformed image $\tilde{I}$.

Differently from the previous method (SM), standard values for regularizing factor λ are set (e.g. $\lambda = 10^{-2}$). Moreover, since in this case the objective is to exactly retrieve the surface S_{IPM} that generates $\tilde{I}$, BCs can be freely set without the need of using the special attentions paid in the case of SM. Also in this case, a planar normal map is used as initialization. Minimization allows to retrieve a normal map Φ_{IPM}^{temp} from which, using Eqn. 2.6, a surface S_{IPM}^0 is defined.

2.4. Main Reconstruction Problem

Depending on the adopted method (SM or IPM), two different rough surfaces are available: S_{SM} and S_{IPM}. From such surfaces, it is possible to compute two normal maps Φ_{SM}^0 and Φ_{IPM}^0. Such normal maps are used as initialization for the final surface reconstruction using Eqn. 2.5, i.e. for solving the so called *main reconstruction problem*. This consists of generating two new normal maps Φ_{SM} and Φ_{IPM}, again using Gauss Seidel with SOR. Finally, the two corresponding surfaces S_{SM} and S_{IPM} are obtained in a way totally similar to that described for SM (i.e. by minimizing Eqn. 2.6). The whole process is summarized in Fig. 5.

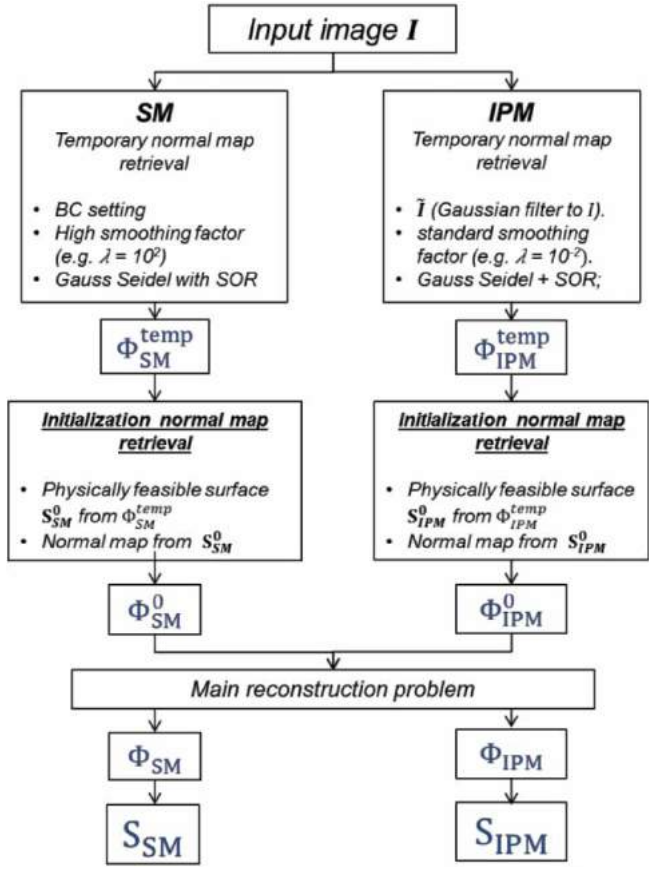

Fig. 5: Flow chart for the whole reconstruction process.

3. CASE STUDIES

The complete procedure described in Section 2, comprising the two methods meant to provide an appropriate initialization to the main reconstruction problem, have been tested on an extensive set of case studies. For this purpose, the procedure has been implemented using Matlab® environment. In the following sections some illustrative case studies are shown in order to highlight strengths and weaknesses of the proposed approach. Results are also

Fig. 6: (a) Input image; (b) ground truth; (c) resulting surface starting from a planar initialization.

compared with the ones obtained using alternative techniques.

3.1. Full 3D: Buddha Statuette

The first case study consists of a full 3D Buddha statuette under frontal illumination. As shown in Fig. 6a, the input image may be considered a mixture of several levels of spatial frequency; this can be observed, for instance, in the smooth shape of the belly (low frequency) and in the folds of the garment (high frequency).

Fig. 6b and Fig. 6c represent the ground truth surface and the result obtained using traditional SFS minimization method with a planar initialization are shown [34].

In Fig. 7, the two initialization surfaces obtained with the proposed methods are shown. In this case, even if both the surfaces are obviously smoothed, the shape obtained using the IPM may be considered qualitatively better than the one reconstructed using the SM.

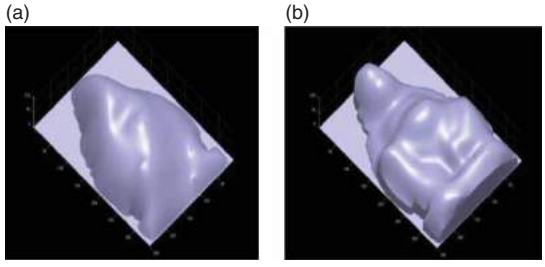

Fig. 7: (a) Initialization obtained by SM - S^0_{SM}; (b) initialization obtained by IPM - S^0_{IPM}.

The surfaces obtained at the end of the whole reconstruction process are shown in Fig. 8a and Fig. 8b. Although the shape of the belly is better defined in the surface of Fig. 8a all other details (e.g. details of the face, shape of the garment) are significantly better represented in the surface of Fig. 8b.

It needs to be pointed out that some regions are not correctly retrieved in the reconstructed surface: for instance, the statuette's base is not reproduced satisfactorily. However, as expected, a better final reconstruction than the one obtained with traditional SFS and planar initialization is obtained by initializing with an appropriate surface (i.e. with S^0_{IPM}).

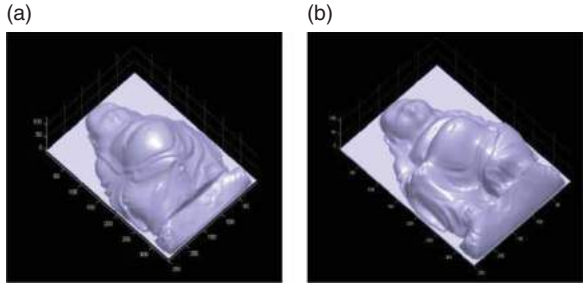

Fig. 8: (a) Final surface obtained by SM - S_{SM}; (b) final surface obtained by IPM - S_{IPM}.

3.2. Bas Reliefs: Golf Ball and Tyrannosaur

The first bas relief-like case study refers to the reconstruction of a surface resembling a golf ball, starting from its synthetic image (actually, the surface has been obtained by down-scaling along the vertical direction the 3D model of half of a golf ball). It is important to remark that, albeit the surface is regular and may appear quite simple to retrieve, actually the task is not that simple, due to the coexistence of high and low frequency geometries.

In Fig. 9 the original image, its ground truth surface and the one obtained using traditional SFS minimization method with a planar initialization are shown [34].

In Fig. 10, the two initialization surfaces, respectively obtained using SM and IPM, are shown. The final surfaces (see Fig. 11) are very similar; the only (barely visible) difference is that the surface in Fig. 11c and Fig. 11d appears slightly smoother than the one in Fig. 11a and Fig. 11b, especially on the top of the shape. In both cases, the retrieved surface is better resembling the expected one than the solution depicted in Fig. 9c.

Moreover, these results are compared with the ones obtained using techniques commonly available in commercial software packages. As mentioned in the introductory section, these techniques consist in generating the relief by directly using as a height map:

Method 1. directly the starting image of the object;
Method 2. the image resulting from derivative-based operators applied to the starting image itself (image embossing);

Fig. 9: (a) Input image; (b) ground truth; (c) resulting surface starting from a planar initialization.

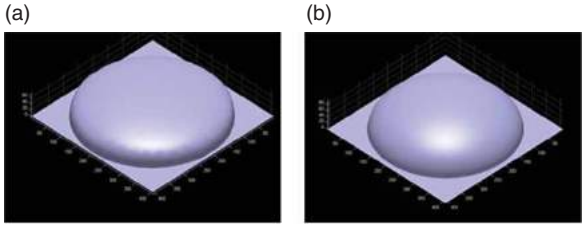

Fig. 10: (a) Initialization obtained by SM - S^0_{SM}; (b) Initialization obtained by IPM - S^0_{IPM}.

Method 3. combination of inflation and *Method 1*;
Method 4. combination of inflation and *Method 2*.

In Fig. 12 the results obtained using such methods are shown; a visual comparison can easily demonstrate that the surfaces obtained by the proposed method are closer to the ground truth.

An additional case study i.e. the image of a bas-relief representing a tyrannosaur (Fig. 13), has been considered in order to assess the effectiveness of the proposed procedure. Since IPM proved to outperform SM, only results obtained by IPM are shown in the rest of the discussion. Moreover *Methods 1* and 2 (see above) are not considered anymore due to their manifest inability to produce satisfactory results. Such a case is quite complex and characterized by a relatively high dimension and, consequently, a large number of unknowns ($> 10^6$). The final retrieved surface (Fig. 13c) looks very similar to the ground truth (Fig. 13b) but, as can be observed in Fig. 14, the same could be said with reference

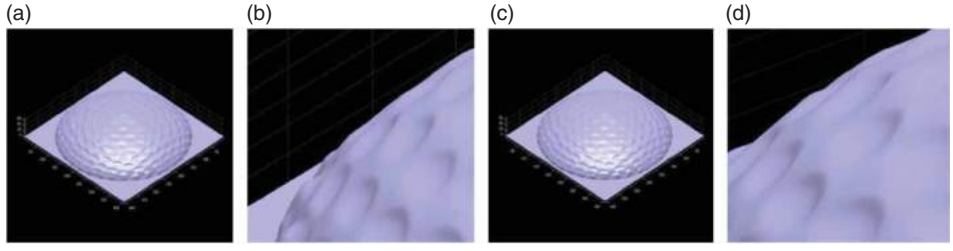

Fig. 11: (a) Final surface obtained by SM - S_{SM}; (b) close detail of S_{SM}; (c) final surface obtained by IPM - S_{IPM}; (d) close detail of S_{IPM}.

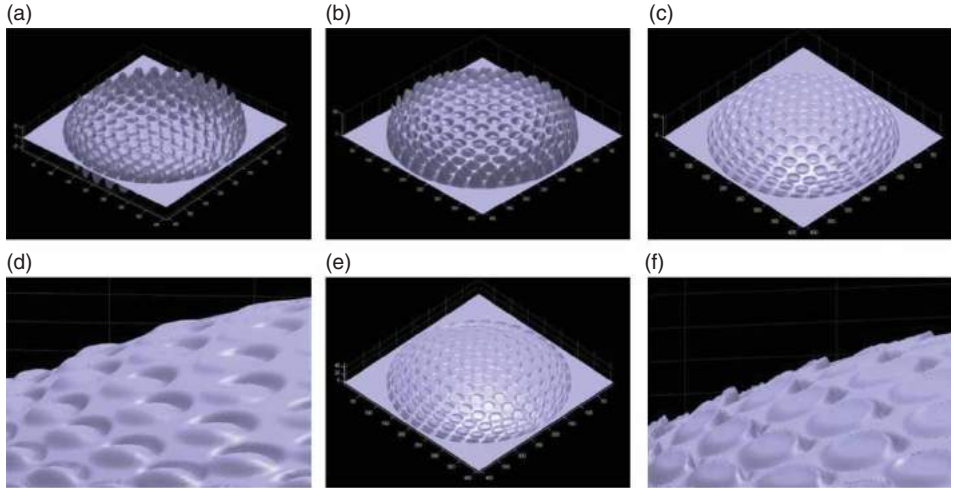

Fig. 12: (a) Surface obtained using *Method 1*; (b) Surface obtained using *Method 2;* (c) Surface obtained using *Method 3*; (d) close detail of surface obtained using *Method 3*; (e) Surface obtained using *Method 4*; (f) close detail of surface obtained using *Method 4*.

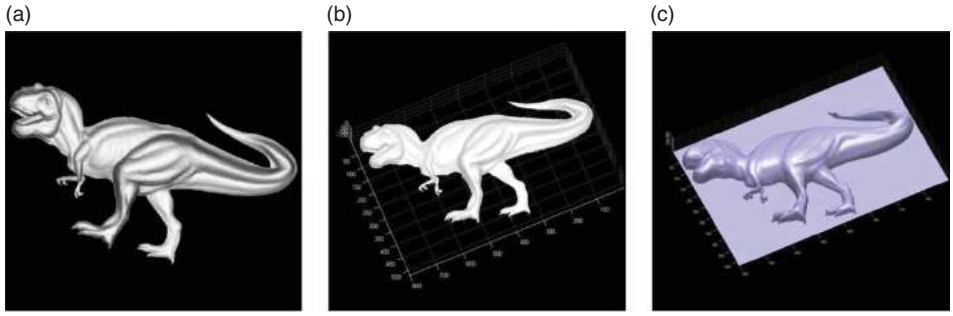

Fig. 13: (a) Input image; (b) ground truth; (c) surface obtained using the proposed method (IPM).

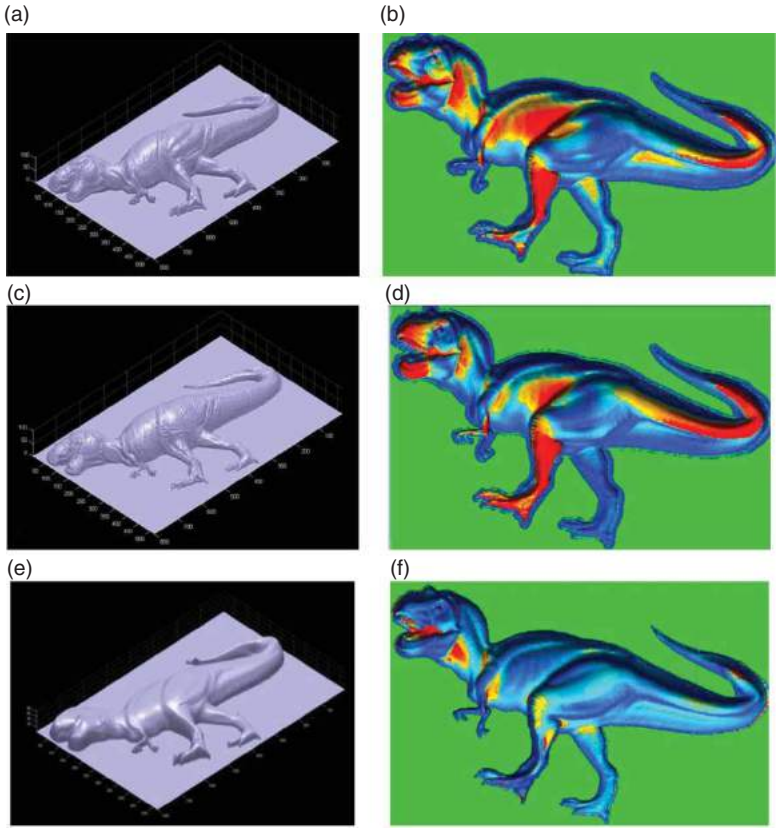

Fig. 14: (a) Surface obtained using *Method 3*; (b) differences between the surface obtained using *Method 3* and the ground truth; (c) surface obtained using *Method 4*; (d) differences between the surface obtained using *Method 4* and the ground truth; (e) surface obtained using the proposed method - IPM; (f) differences between the surface obtained using the proposed method and the ground truth.

to the surfaces obtained by means of *Method 3* and *Method 4*.

Since the ground truth is available for this case study, a color map of the absolute distance between the analyzed surface and the ground truth (Fig. 14) has been produced in order to highlight the existing differences. The analysis of Fig. 14 clearly points out that the proposed method significantly outperforms *Method 3* and *Method 4*.

4. CONCLUSIONS AND FUTURE WORK

This work proposes a novel method for accurate reconstruction of digital bas-relief from single image using a new SFS-based technique with interactive initialization. The described approach is meant to speed up and increase the accuracy of the design phase of products characterized by stylistic content and organic shapes such the ones employed, for instance, for fashion accessories.

The reconstruction is performed first by interactively setting a number of user selected boundary conditions; then, by applying two alternative approaches, devised in order to retrieve a surface representing a rough version of the desired final shape. Such surfaces are finally used as initialization for a SFS-based reconstruction algorithm based on Gauss-Seidel iteration with Successive Over Relaxation. Though a number of solutions can be found both in scientific literature and in commercial software packages, a number of limitations still persist mainly due to the necessity of excessive user interaction and/or to the fact that the final surface only visually resembles the desired one.

In the proposed method only a limited user interaction is needed in order to allow the retrieval of more accurate surfaces. The method, developed using Matlab® programming environment, was tested against a series of case studies and proved to be effective in providing digital bas-reliefs whose shapes satisfactorily reproduces the original (or expected) ones.

The main limitation of the proposed procedure lies in the possibility of running into an over-smoothing effect (see Fig. 11 and Fig. 13). In order to achieve less smoothed surfaces, however, it is not recommended to reduce the regularization factor λ for smoothness constraint; in fact, excessively low values of this factor may produce surfaces very far from the expected ones. This problem can be partially mitigated (at least from a visual point of view) by using a combination of the proposed procedure with either direct image height map or image embossing.

In Fig. 15 the surface obtained with the proposed method and the one obtained by combining it with the original image treated as a height map are shown.

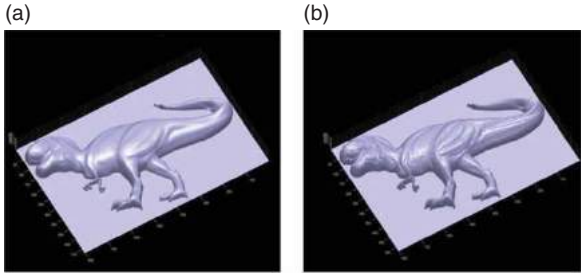

Fig. 15: (a) Surface obtained using the proposed method; (b) Surface obtained by combining the surface (a) with the original image treated as a height map.

Future work will be addressed to increase the number of test cases, with particular regard to real world and noisy images; this will allow to point out possible issues and to consider appropriate improvements. For instance, though in the scientific literature it is one of the most widely used due to its simplicity and speed, Gauss-Seidel based minimization method is probably not the best option for solving linear, constrained optimization problems. In fact, this technique is typically usable for unconstrained problems. Accordingly, future work will be devoted to investigate the performance of alternative minimization algorithms, such as Interior Point one.

Furthermore, the possibility of incorporating feature recognition, in order to speed up the reconstruction of primitives (if any) represented in images will be investigated.

Finally, additional exploitation of obtained results will also be possible in the field of reconstruction of 3D models for tactile exploration starting from single images. In particular, the bas-relief like surfaces obtained using the described technique could be superimposed to a starting flat-layered 3D model representing the scene structure [3,28].

ACKNOWLEDGEMENTS

The authors wish to acknowledge the Tuscany Region (Italy) for co-funding the *T-VedO* project (PAR-FAS 2007-2013), which originated and made possible this research.

REFERENCES

[1] Bhuruth, M.; Evans, D.: Block iterative methods for the nine-point approximation to the convection-diffusion equation, International journal of computer mathematics, 61, 1996, 321–335. http://dx.doi.org/10.1080/00207169608804519

[2] Brooks, M. J.; Horn, B. K.: Shape and source from shading, 1985.

[3] Carfagni, M.; Furferi, R.; Governi, L.; Volpe, Y.; Tennirelli, G.: Tactile representation of paintings: An early assessment of possible computer based strategies, Progress in Cultural Heritage Preservation, Lecture Notes in Computer Science 7616 LNCS, 2012, 9. http://dx.doi.org/10.1007/978-3-642-34234-9_26

[4] Daniel, P.; Durou, J.-D.: From deterministic to stochastic methods for shape from shading, in: Proc. 4th Asian Conf. on Comp. Vis, Citeseer, 2000, 1–23.

[5] Di Angelo, L.; Di Stefano, P.: Bilateral symmetry estimation of human face, International Journal on Interactive Design and Manufacturing (IJIDeM), 2012, 1–9. http://dx.doi.org/10.1007/s12008-012-0174-8

[6] Durou, J.-D.; Falcone, M.; Sagona, M.: Numerical methods for shape-from-shading: A new survey with benchmarks, Computer Vision and Image Understanding, 109, 2008, 22–43. http://dx.doi.org/10.1016/j.cviu.2007.09.003

[7] Frankot, R. T.; Chellappa, R.: A method for enforcing integrability in shape from shading algorithms, Pattern Analysis and Machine

Intelligence, IEEE Transactions on, 10, 1988, 439–451. http://dx.doi.org/10.1109/34.3909

[8] Governi, L.; Furferi, R.; Puggelli, L.; Volpe, Y.: Improving surface reconstruction in Shape from Shading using easy-to-set boundary conditions, International Journal of Computational Vision and Robotics, forthcoming 2013.

[9] Horn, B. K.: Height and gradient from shading, International journal of computer vision, 5, 1990, 37–75. http://dx.doi.org/10.1007/BF00056771

[10] Horn, B. K.: Shape from shading: A method for obtaining the shape of a smooth opaque object from one view, 1970.

[11] Huang, R.; Smith, W. A.: Structure-preserving regularisation constraints for shape-from-shading, in: Computer Analysis of Images and Patterns, Springer, 2009, 865–872. http://dx.doi.org/10.1007/978-3-642-03767-2_105

[12] Huang, Z. K.; Zhang, X. W.; Zhang, W. Z.; Hou, L. Y.: A New Embossing Method for Gray Images Using Kalman Filter, Applied Mechanics and Materials, 39, 2011, 488–491. http://dx.doi.org/10.4028/www.scientific.net/AMM.39.488

[13] Igarashi, T.; Matsuoka, S.; Tanaka, H.: Teddy: a sketching interface for 3D freeform design, in: ACM SIGGRAPH 2007 courses, ACM, 2007, 21. http://dx.doi.org/10.1145/1281500.1281532

[14] Ikeuchi, K.; Horn, B. K.: Numerical shape from shading and occluding boundaries, Artificial intelligence, 17, 1981, 141–184. http://dx.doi.org/10.1016/0004-3702(81)90023-0

[15] Kerber, J.; Tevs, A.; Belyaev, A.; Zayer, R.; Seidel, H.-P.: Real-time generation of digital bas-reliefs, Computer-Aided Des. Appl, 7, 2010, 465–478. http://dx.doi.org/10.3722/cadaps.2010.465-478

[16] Kimmel, R.; Bruckstein, A. M.: Tracking level sets by level sets: a method for solving the shape from shading problem, Computer Vision and Image Understanding, 62, 1995, 47–58. http://dx.doi.org/10.1006/cviu.1995.1040

[17] Lee, C.-H.; Rosenfeld, A.: Improved methods of estimating shape from shading using the light source coordinate system, Artificial Intelligence, 26, 1985, 125–143. http://dx.doi.org/10.1016/0004-3702(85)90026-8

[18] Li, Z.; Wang, S.; Yu, J.; Ma, K.-L.: Restoration of brick and stone relief from single rubbing images, Visualization and Computer Graphics, IEEE Transactions on, 18, 2012, 177–187. http://dx.doi.org/10.1109/TVCG.2011.26

[19] Liverani, A.; Leali, F.; Pellicciari, M.: Real-time 3D features reconstruction through monocular vision, International Journal on Interactive Design and Manufacturing (IJIDeM), 4, 2010, 103–112. http://dx.doi.org/10.1007/s12008-010-0093-5

[20] Pentland, A.: Shape information from shading: a theory about human perception, 1988. http://dx.doi.org/10.1163/156856889X00103

[21] Prados, E.; Camilli, F.; Faugeras, O.: A viscosity solution method for shape-from-shading without image boundary data, ESAIM: Mathematical Modelling and Numerical Analysis, 40, 2006, 393–412. http://dx.doi.org/10.1051/m2an:2006018

[22] Remondino, F.; El-Hakim, S.: Image-based 3D Modelling: A Review, The Photogrammetric Record, 21, 2006, 269–291. http://dx.doi.org/10.1111/j.1477-9730.2006.00383.x

[23] Repenning, A.: Inflatable icons: Diffusion-based interactive extrusion of 2d images into 3d models, journal of graphics, gpu, and game tools, 10, 2005, 1–15. http://dx.doi.org/10.1080/2151237X.2005.10129187

[24] Rouy, E.; Tourin, A.: A viscosity solutions approach to shape-from-shading, SIAM Journal on Numerical Analysis, 29, 1992, 867–884. http://dx.doi.org/10.1137/0729053

[25] Stylianou, G.; Lanitis, A.: Image based 3d face reconstruction: a survey, International Journal of Image and Graphics, 9, 2009, 217–250. http://dx.doi.org/10.1142/S0219467809003411

[26] Sun, X.; Rosin, P. L.; Martin, R. R.; Langbein, F. C.: Bas-relief generation using adaptive histogram equalization, Visualization and Computer Graphics, IEEE Transactions on, 15, 2009, 642–653. http://dx.doi.org/10.1109/TVCG.2009.21

[27] Tsai, P.-S.; Shah, M.: Shape from shading using linear approximation, Image and Vision Computing, 12, 1994, 487–498. http://dx.doi.org/10.1016/0262-8856(94)90002-7

[28] Volpe, Y.; Furferi, R.; Governi, L.; Tennirelli, G.: Computer-based methodologies for semi-automatic 3D model generation from paintings, Int. J. Computer Aided Engineering and Technology, forthcoming 2013.

[29] Wang, M.; Chang, J.; Zhang, J. J.: A review of digital relief generation techniques, in: Computer Engineering and Technology (ICCET), 2010 2nd International Conference on, IEEE, 2010, 198–202. http://dx.doi.org/10.1109/ICCET.2010.5485636

[30] Weyrich, T.; Deng, J.; Barnes, C.; Rusinkiewicz, S.; Finkelstein, A.: Digital bas-relief from 3D scenes, ACM Transactions on Graphics (TOG), 26, 2007, 32. http://dx.doi.org/10.1145/1276377.1276417

[31] Worthington, P. L.; Hancock, E. R.: Needle map recovery using robust regularizers, Image and Vision Computing, 17, 1999, 545–557. http://dx.doi.org/10.1016/S0262-8856(98)00173-5

[32] Wu, J.; Martin, R.; Rosin, P.; Sun, X.-F.; Langbein, F.; Lai, Y.-K.; Marshall, A.; Liu, Y.-H.: Making bas-reliefs from photographs of human faces, Computer-Aided Design, 45, 2013, 12. http://dx.doi.org/10.1016/j.cad.2012.11.002

[33] Wu, T.-P.; Sun, J.; Tang, C.-K.; Shum, H.-Y.: Interactive normal reconstruction from a single image, ACM Transactions on Graphics (TOG), 27, 2008, 119. http://dx.doi.org/10.1145/1409060.1409072

[34] Zhang, R.; Tsai, P.-S.; Cryer, J. E.; Shah, M.: Shape-from-shading: a survey, Pattern Analysis and Machine Intelligence, IEEE Transactions on, 21, 1999, 690–706. http://dx.doi.org/10.1109/34.784284